

## A FLAVOR OF KLOE\*

JULIET LEE-FRANZINI

Laboratori Nazionali di Frascati dell'INFN Frascati, Rome, Italy

PAOLO FRANZINI

Sezione di Roma1 dell'Istituto Nazionale di Fisica Nucleare, Roma, Italy

*(Received July 2, 2007)*

This paper is a simple, quick guide to KLOE, the flagship experiment of INFN's  $\phi$ -factory DAΦNE at Frascati. KLOE's design principles, properties, its physics accomplishments and its impact on "flavor physics", are described in terms comprehensible to non specialists.

PACS numbers: 11.30.Er, 13.20.Eb, 13.20.-v, 14.40.Aq

**1. Introduction**

In late 1988 the Italian Institute for Nuclear Physics, INFN, decided to construct an  $e^+e^-$  collider meant to operate around 1020 MeV, the mass of the  $\phi$ -meson. The  $\phi$ -meson decays mostly to kaons, neutral and charged, in pairs. The  $\phi$  production cross-section peaks at about  $3\mu\text{barns}$ .  $\phi$ -mesons decay  $\sim 49\%$  of the time into  $K^+K^-$  pairs and  $34\%$  of the time into  $K^0\bar{K}^0$  pairs. Even with a modest luminosity,  $\mathcal{L} = 100\mu\text{b}^{-1}/\text{s}$ , hundreds of kaon pairs are produced per second. This collider, called a  $\phi$ -factory and christened DAΦNE, is located at the Laboratori Nazionali di Frascati, INFN's high energy physics laboratory near Rome [1].

*1.1. DAΦNE*

The DAΦNE layout is shown in Fig. 1. The heart of the collider are two storage "rings" in which 120 bunches of electrons and positrons are stored. Each bunch collides with its counter part once per turn, minimizing the perturbation of each beam on the other. Electrons and positrons are injected in the rings at final energy,  $\sim 510\text{ MeV}$ . Electrons are accelerated to

---

\* Presented at The Final EURIDICE Meeting "Effective Theories of Colours and Flavours: from EURODAΦNE to EURIDICE", Kazimierz, Poland, 24–27 August, 2006.

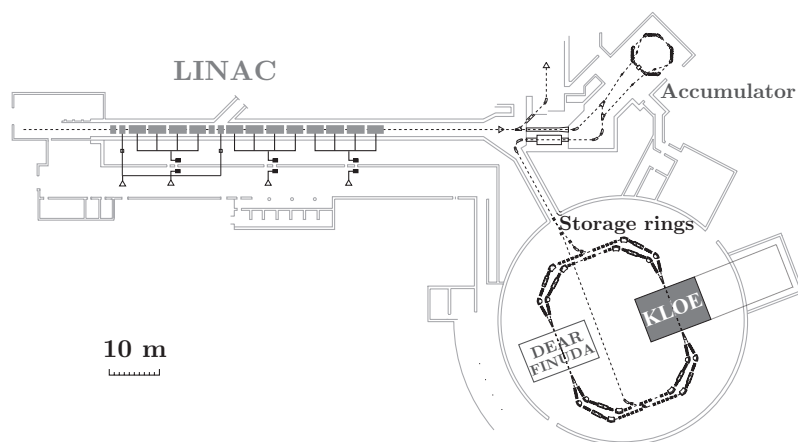


Fig. 1. The DAΦNE complex.

final energy in the Linac, accumulated and cooled in the accumulator and transferred to a single bunch in the ring. Positrons require first accelerating electron to about 250 MeV to an intermediate station in the Linac, where positrons are created. The positrons then follow the same processing as electrons. Since the stored beam intensities decay rapidly in time, the cycle is repeated several times per hour. A collider is characterized by its luminosity  $\mathcal{L}$  defined by: event rate =  $\mathcal{L} \times$  cross-section, beam lifetime and beam induced radiation background.

The latter is large for short lifetimes, which also result in the average luminosity being smaller than the peak value, in a word, lower event yield and large, variable background. DAΦNE is housed in the ADONE building at LNF, see Fig. 2.



Fig. 2. The Adone building.

### 1.2. KLOE

INFN soon realized that a state-of-the-art detector was needed to collect data at DAΦNE, from which physics results would materialize. Thus a couple of years later, in summer 1991, the KLOE Collaboration was initiated, though it was not formally approved nor fully funded for another couple of years, because the authorities had not envisioned fully the magnitude of KLOE. By late 1998 however, KLOE was designed, constructed, completely tested, and the humongous KLOE detector, complete with all of its electronics for signal processing, event gathering and transmission, was moved from its own especially built assembly hall onto the newly commissioned DAΦNE's South Interaction Region. In the subsequent seven years KLOE, after beginning with a trickle of beam, by 2006, had produced data of such precision that the kaon, the first fundamental particle to introduce the concept of “flavor” in our current way of thinking, got its definitive XXI century portrait re-mapped with high precision, 60 years after its discovery.

The KLOE saga, with its concomitant joys and travails, would be an entertaining tale that should be written up somewhere. Our purpose in this paper, instead, is to give the non-specialist reader a “flavor” of the KLOE experiment, in order to better appreciate the role that a complete experiment such as KLOE plays in pushing forward the physics frontier.

## 2. Detector

The KLOE detector has a giant inner core, approximately 125 meters cubed, see Fig. 3, and was built in Frascati in the KLOE assembly building, see Fig. 4. It is on the same scale and complexity as the “general purpose detectors” of its time that were operating at the world’s foremost laboratories such as LEP at CERN. If we consider that LEP operated at about one hundred times DAΦNE’s energy, producing much more energetic particles and with correspondingly greater multiplicities, KLOE’s large size would seem unwarranted. We shall see, however, that while KLOE’s complexity was necessitated by its intent of being a definitive high precision experiment, its size, instead, was dictated by the quirk of one of the two neutral kaons, called the  $K_L$ , of living an extraordinarily long time (for short lived particles), about 51 nanoseconds. Kaons from  $\phi$ -mesons decaying at rest travel at approximately one fifth of the speed of light. This low speed is a great bonus for many reasons. However, the mean path travelled by a  $K_L$ -meson,  $L_{K_L} = \gamma\beta c\tau$  is 3.48 m. Thus if we want a detector which can catch  $1 - 1/e = 63\%$  of all decaying neutral long-lived kaons, it must have a radius of some three and a half meters. We compromise on two meters and catch some 40% of those decays. Less than that in fact, since some volume

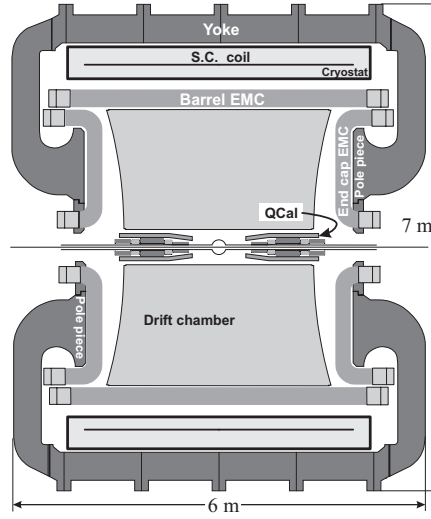


Fig. 3. Cross-sectional view of the KLOE experiment, showing the interaction region, the drift chamber (DC), the electromagnetic calorimeter (EMC), the superconducting coil, and the return yoke of the magnet.

is inevitably lost around the beam interaction point, IP, and some more is lost at the outer edge, in order to be able to recognize the nature of the decays close to it.



Fig. 4. KLOE Assembly Hall. The KLOE control room is on the top floor. The Adone cupola is just visible behind.

### 2.1. Drift chamber

Catching a decay really means observing the decay products or particles. Charged particle travelling in a medium, a gas, undergo repeated collisions with electrons. As a result a string of ion pairs marks its passage. This is how KLOE came to build the largest drift chamber, DC, in high-energy

physics. A DC is a gas filled chamber traversed by a large number of wires, some kept at +2000 volt, anode wires, some at ground. Electrons of the ion pairs created along the particle trajectory drift to the positive voltage wires. Thanks to an avalanche multiplication mechanism a detectable signal appears at the wire end. Measuring the drift time locates the distance of the track from the anode wires and ultimately we can reconstruct the trajectory of the particles. Sophisticated electronics mounted at the wire's end senses the tiny signals. The KLOE DC has  $\sim 52000$  wires, about 12500 of them are sense wires, the remaining ones shape the electric field in 12500 small ( $2 \times 2$ ,  $3 \times 3$  cm<sup>2</sup>) cells. For a particle crossing the entire chamber we get dozens of space points from which we reconstruct a track. The DC is surrounded by a superconducting coil that produces a magnetic field of  $\sim 0.5$  Tesla. The particle trajectories curl up and we determine the particle's momentum from the curvature of its track with a fractional accuracy of  $\sim 0.4\%$ . The spatial resolution is well below 200  $\mu\text{m}$  in the " $\phi$ -coordinate" [2].

## 2.2. Electromagnetic calorimeter

The neutral decay products of the  $K_L$ 's, its short-lived partner  $K_S$  (lifetime  $\sim 89$  picoseconds), and of those of their charged brethren, the  $K^\pm$ 's which we need to detect are photons, either directly produced or from the decay of neutral pions into two photons. Photons do not ionize, but interact with matter by photoelectric effect, Compton scattering and for energies larger than a few MeV (as in most of our cases) by electron positron pair production. Electrons and positrons in turn radiate photons when traversing matter, a process quite similar to pair-production. Thus, one readily imagines that a photon, or an electron for that matter, traveling through dense, high  $Z$  matter, repeatedly undergoes radiation and pair production in cascade, until all its energy is expended in a so called shower of  $e^+e^-$  and photons. Detection of these particles and their energy measures the original photon's (or electron's) energy. This is done with a "calorimeter", which also usually pin points the position of the electromagnetic cascade (or shower) as well.

The KLOE calorimeter EMC, is a sampling calorimeter. It is made of lead passive layers that accelerate the showering process and of scintillating fiber sensing layers. Energy densities are sampled at different depth along the shower development. The basic structure of the KLOE calorimeter is a composite of very thin, 1 mm, grooved Pb layers between which are embedded 1 mm diameter scintillating fibers.  $\sim 200$  Pb-fiber layers are used. The high ratio of active material to radiator and the very fine subdivision result in better energy resolution. In addition, the special care in design and assembly of the Pb-fiber composite ensures that the light propagates along

the fiber in a single mode, resulting in a greatly reduced spread of the light arrival time at the fiber ends. Photomultiplier at both fiber ends transform this light into electric pulses. Their amplitude gives the amount of energy deposit. The arrival times locates the position of the shower to  $\mathcal{O}(1)$  cm accuracy. The resulting material has a radiation length  $X_0$  of 1.5 cm. 30 cm or  $15 X_0$  fully contain a shower of 500 MeV. About 5 000 photomultiplier tubes view the  $24 + 32 + 32$  modules into which the calorimeter is subdivided.

The calorimeter material is formed into a barrel, aligned with the beams and surrounding the DC. In additions two end plugs, draped over the magnet pole pieces hermetically close the calorimeter  $\sim 98\%$  of  $4\pi$ , see Fig. 3. The KLOE calorimeter, EMC, with time resolution of the order of 54 picoseconds for a one GeV photon, is jocularly referred to as “the fastest calorimeter in the West”. The energy resolution of KLOE is also excellent, of the order of 5.7% for a one GeV photon [3].

### 2.3. Beam pipe

At DAΦNE the electron and positron beams collide almost head on,  $\theta = \pi - 25$  mrad.  $\phi$ -mesons are, therefore, produced with  $\sim 13$  MeV/ $c$ , in the horizontal plane, toward DAΦNE’s center. The  $K_S$ ’s with its lifetime of  $\sim 89$  ps or 6 mm path length, emit secondary particles almost isotropically from the interaction point (IP). At the IP the beam pipe is built of a Al-Be alloy 1 mm thick and shaped as a 10 cm radius sphere, Fig. 5. The  $K_S$  amplitude is reduced by a factor of  $\sim 5$  000 at the sphere surface. Regeneration,  $K_L \rightarrow K_S$ , can be neglected in the crucial interference region.

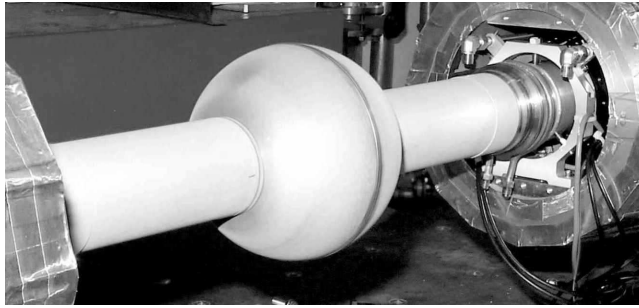


Fig. 5. Beam pipe at the KLOE interaction region. Just visible on either side are the final focus quad ends.

### 2.4. Trigger

The total  $e^+e^-$  cross-section at 1020 MeV is  $\mathcal{O}(100) \mu\text{b}$ , of which only  $3 \mu\text{b}$  is due to  $\phi$ -production. In DAΦNE the collision frequency reaches up to  $3.68 \times 10^8$  Hz. A trigger is necessary to fire up the electronics, to process signals from some 20 000 detector elements, only when something

interesting happened. We want  $\phi$  decays, and a fraction  $e^+e^- \rightarrow e^+e^-$  (Bhabha) or  $\gamma\gamma$  events, for  $\mathcal{L}$  measurement and for continuous monitoring and calibration of KLOE. We also wish to ignore cosmic rays descending into KLOE from the heavens. An elaborate electronic logic system rapidly recognizes topologies and energy releases of interest, providing the signal or “trigger” that something interesting happened. The KLOE trigger is based on isolated energy releases in the calorimeter and the presence of  $\sim 15$  hits in the DC within a time window of  $\sim 250$  ns from beam crossing. This trigger, called Level 1, initiate conversion in the front-end electronics modules, which are subsequently read out following a fixed time interval. A second level trigger, requiring  $\sim 120$  hits within a  $1.2\mu\text{s}$  window in the DC validates the trigger. The KLOE trigger also recognize and ignores cosmic ray events [4]. A valid trigger initiates read out. The trigger system also provides a fast measurement of the DAΦNE luminosity. A precision measurement of the luminosity is obtained off line from Bhabha events [5].

### 2.5. Data acquisition

At a luminosity of  $\sim 100\mu\text{b}^{-1}/\text{s}$ , events worth keeping occur at about 2 200 Hz. Of these  $\sim 300$  Hz are from  $\phi$  decays. All digitized signals from the calorimeter, drift chamber, calibration and monitoring systems are fed from the electronics that sit on platforms mounted on the KLOE iron yoke, via fiber optics to the KLOE computers in the next building. In the nearby KLOE control room one can see real time displays of reconstructed charged tracks traversing the DC and photons depositing energy clusters in the calorimeter.

The events are reconstructed, meaning that charged tracks and energy deposits that occurred at the same instant in time on the various subcomponents of KLOE using constantly updated calibration files that monitor both the time and energy scales, are associated together, properly labeled and packed into a unique file. Furthermore, background hits that accidentally occurred during the time an event time window is open, are also recorded such that these hits can be added on (superimposed) on the simulated KLOE events (MC). The KLOE MC simulation program reproduces the KLOE geometry, physical responses and trigger requirements extremely well, but of course cannot foretell the moment to moment variation of background.

All raw data, background, reconstructed and MC events are recorded on tape. KLOE has a huge tape library of  $\sim 800$  TB capacity [6]. At reconstruction time, events are classified in broad categories or “streams”. Data summary tapes are produced as a separate procedure. Any of the KLOE analyses, even after event reconstruction is quite complex. It includes making data summary “tapes” and extensive modeling of the detector response.

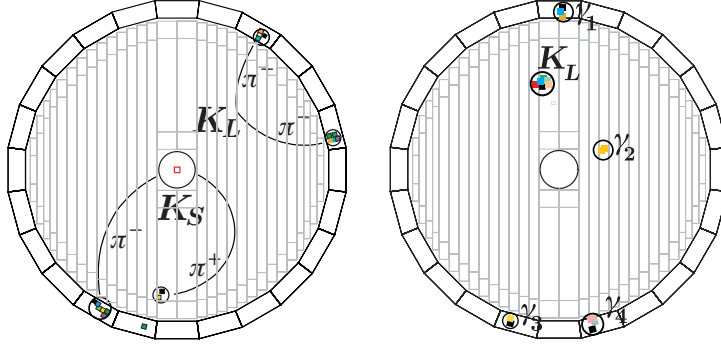


Fig. 6.  $K_S K_L$  events in KLOE. Left: both  $K_L$  and  $K_S$  decay to charged pions  $\pi^+ \pi^-$ . Color patches indicate energy in the calorimeter. Right: 5 neutral particles.  $\gamma_1$  through  $\gamma_4$  are showers from 4 photons from  $K_S \rightarrow \pi^0 \pi^0 \rightarrow 4\gamma$ . The  $K_L$ -mesons reaches the calorimeter before decaying. It literally crashes in the EMC, producing a huge energy release.

This requires generation of large number of Monte Carlo (MC) events for each studied process. Both data and MC summaries ( $\sim 80$  TB) are cached on disk for analysis [7].

### 2.6. $K_L$ path

The production of  $K_S K_L$  pairs in  $\phi$ -decays together with the excellent timing accuracy of the KLOE EMC allows us to locate  $K_L \rightarrow \pi^0 \pi^0$  decay point, in the terrible jargon of today's physicists, a “neutral vertex”, to accuracies of  $\mathcal{O}(3)$  mm, as illustrated in Fig. 7. This procedure is of fundamental importance in most of KLOE measurements.

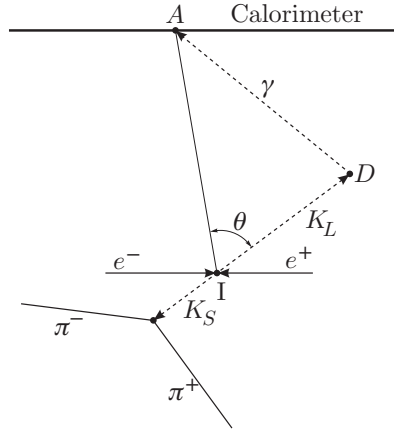


Fig. 7.  $D$  is the  $K_L \rightarrow \pi^0 \pi^0 \rightarrow 4\gamma$  decay point. The  $K_L$  path is obtained from the time for each photon to arrive at the calorimeter,  $t(I \rightarrow A)$ , and the  $K_S$  direction.

2.7. The  $K_S$  beam

The two neutral kaon state from a  $\phi$ -decay is given, in the  $\phi$  rest frame, by

$$\begin{aligned} |i\rangle &= \frac{|K^0, \mathbf{p}\rangle |\bar{K}^0, -\mathbf{p}\rangle - |\bar{K}^0, \mathbf{p}\rangle |K^0, -\mathbf{p}\rangle}{\sqrt{2}} \\ &= \frac{|K_S, \mathbf{p}\rangle |K_L, -\mathbf{p}\rangle - |K_L, \mathbf{p}\rangle |K_S, -\mathbf{p}\rangle}{\sqrt{2}}. \end{aligned} \quad (1)$$

Therefore, observation of a  $K_L(K_S)$  decay ensures the presence of a  $K_S(K_L)$  meson, traveling in the opposite direction. This provides the unique opportunity of preparing a pure  $K_S$ -beam. A pure  $K_L$  beam can thus also be defined, although most experiments accomplish the same by simply waiting for the  $K_S$ -amplitude to die away. We refer to the process of defining a  $K_S$  or  $K_L$  sample as tagging: observation of a  $K_L(K_S)$  decay tags the presence of a  $K_S(K_L)$  meson of known momentum  $\mathbf{p}$ . Because of the exceptional timing capabilities of the KLOE EMC and the slowness of the kaons from  $\phi$ -decays, KLOE tags  $K_S$ -mesons in a unique way. As already mentioned, kaons have a velocity  $\beta = 0.2162$  in the  $\phi$  frame and  $\beta=0.193$  to  $0.239$  in the lab and 60% of them reach the calorimeter in a time of at least 31 ns.  $K_L$ -mesons interact in the calorimeter with an energy release up to their mass, 497 MeV. For an energy release of 100 MeV KLOE has a time resolution of  $\sim 0.3$  ns, *i.e.* a velocity accuracy of  $\sim 1\%$ . The accuracy in measuring the  $K_L$  velocity, before exact determination of the collision time, is shown in Fig. 8.

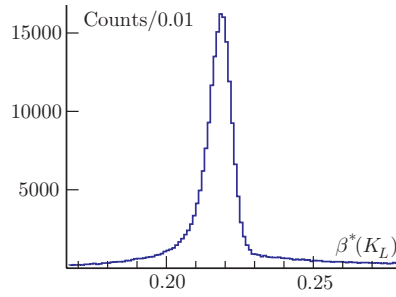


Fig. 8.  $K_L$  velocity in  $\phi$ -frame from time of flight (before exact determination of the collision time).

In KLOE, we call a  $K_L$  interaction in the EMC a “k-crash”. Note that the above error on  $\beta(K_L)$  corresponds to an error on the kaon energy of  $\sim 0.25$  MeV or 0.5 MeV for the collision energy, with just one event. We use this method, together with  $e^+e^- \rightarrow e^+e^-$  events to monitor the DAΦNE energy and energy spread.

### 3. Kaon physical parameters and decays

Since the kaon's discovery about sixty years ago, knowledge of its properties, from masses, lifetimes, and how often each species decays into to which particles, has been accumulated piecemeal literally over hundreds of individual experiments, performed at various laboratories all over the world. Each experiment has its own peculiarity, contingent upon the particle beam available and its own equipment's acceptance range, which can result in highly accurate measurements from a statistical point of view (namely based on thousands of data events) but with hidden corrections peculiar to it perhaps unknown even to its authors. The particle physics "self-nominated authority" in charge of compiling the results, often adopt a "democratic" way of weighing the various results according to their nominal errors and literally applying a fudge factor when faced with two inconsistent measurements. While this procedure skirts the problems of judging the relative accuracy of the results obtained over times, it sometimes ends up with a hodge-podge of inconsistent results forced into a mold of dubious scientific validity.

The mission of KLOE is to measure most, if not all, of the properties of the kaon system to high accuracy, with a single detector simultaneously. Moreover radiation is always present and calculating its effects involves cancellation of infinities. Only if experimental answers are fully inclusive with respect to radiation, can they be compared with calculation in a model. Most branching ratios reported in the past have been very vague on this point. KLOE has been particularly attentive to the inclusion of radiation.

KLOE can accomplish the said goal because as described before, *(i)*, it has available tagged, pure kaon beams (the only  $K_S$  one) of precisely known momenta (known event by event, from kinematic closure) and *(ii)*, of known flux, the number created of each specie, *(iii)*, and catches all the decay products hence determine the fractions of decays into different channels. In short KLOE can measure each kaon specie's total decay rate  $\Gamma$ , the inverse of which is the lifetime, and its fractions of decay into different channels, called branching ratio, BR.

#### 3.1. Masses

Kaons masses are about 500 MeV, very close to one half the  $\phi$ -meson mass, known to an accuracy of  $0.019/1019.460 \sim 2 \times 10^{-5}$ , by the use of the  $g$ -2 depolarizing resonances, [8]. In KLOE we use the  $K_S$  decay into  $\pi^0\pi^0$  and  $\pi^+\pi^-$  routinely to monitor the EMC and DC performance. Measuring the  $K_S$  mass requires measuring  $M(\phi) - 2M(K^0) = 12.05$  MeV, corresponding to  $p(K^0) = 110.2$  MeV. Given the billions of  $K_S \rightarrow \pi^+\pi^-$  decays available in KLOE, the statistical error can be arbitrarily small. The accuracy is ultimately limited by uncertainties in the calculations of radiative corrections. KLOE measures  $M(K_L) = 497.583 \pm 0.021$  MeV [9].

### 3.2. $K^0$ lifetimes

Precision measurements of the lifetime of neutral kaons, especially those with many multibody decay modes is particularly difficult since it is in general not possible to prepare monochromatic beams of neutral particles nor to stop them. KLOE enjoys the availability of such monochromatic beams. While the  $K_S$  lifetime, for many obvious reasons, is quite well known,  $(0.8958 \pm 0.0005) \times 10^{-10}$  s, this is not the case for the  $K_L$  lifetime. KLOE can measure the lifetime by observing the time dependence of the decay frequency to a single mode. Because of tagging, the lifetime can also be obtained by simply counting the total number of decays in a given time interval from a known  $K_L$  sample.

We have collected a sample of  $\sim 14$  million  $K_L \rightarrow \pi^+ \pi^- \pi^0$  decays over a 6–26 ns interval ( $\sim 40\%$  of the  $K_L$  lifetime). A fit of the proper time distribution gives  $\tau_{K_L} = 50.92 \pm 0.30$  ns [10]. From the second method, using  $\sim 2$  million  $K_L$  decays to all major channels, KLOE finds  $\tau_{K_L} = 50.72 \pm 0.36$  ns. The two determinations are in agreement and are almost entirely uncorrelated [11]. The combined result is  $50.84 \pm 0.23$  ns, compared to  $51.54 \pm 0.44$  ns from 1972.

### 3.3. $K^\pm$ lifetime

The measurements of the  $K^\pm$  lifetime listed in the PDG compilation [8] exhibit poor consistency. The PDG fit has a confidence level of  $1.5 \times 10^{-3}$ , and the error on the recommended value is enlarged by a scale factor of 2.1. KLOE can measure the decay time for charged kaons in two ways. The first method is to obtain the proper time from the kaon path length in the DC. Our preliminary value for the lifetime is  $\tau_{K^\pm} = 12.367 \pm 0.044 \pm 0.065$  ns, where the first error is statistical and the second systematic.

The second method is based on the precise measurement of the arrival times of the photons from  $K^\pm \rightarrow \pi^\pm \pi^0$  decays and the determination of the decay point from the track vertex in the DC. It is near completion. Both methods provide results accurate to the level of 0.1%.

### 3.4. $K_S$ decays

As already mentioned, central to KLOE's  $K_S$  studies is the use of  $K_L$ -crash tag: the position of the  $K_L$  crash, together with the kinematics of the  $\phi \rightarrow K_S K_L$  decay, determines the trajectory of the  $K_S$  with a momentum resolution of approximately 1 MeV and an angular resolution of better than  $1^\circ$ . Using  $K_L$ -crash tag KLOE was able to measure the  $K_S$  branching ratios whose values span six orders of magnitude.

$K_S \rightarrow \pi^+\pi^-(\gamma), \pi^0\pi^0$  — the  $K_S$  decays overwhelmingly (99%) into two pions:  $\pi^0\pi^0$  and  $\pi^+\pi^-$ . The ratio of the charged decay mode to that of the neutral  $\mathcal{R}_\pi \equiv \Gamma(K_S \rightarrow \pi^+\pi^-(\gamma))/\Gamma(K_S \rightarrow \pi^0\pi^0)$  is a fundamental parameter of the  $K_S$  meson. It is used in the extraction of values for phenomenological parameters of the kaon system, such as the differences in magnitude and phase of the  $I = 0, 2$   $\pi\pi$  scattering amplitudes. It and the corresponding ratio from the  $K_L$  together determine the amount of direct CP violation in  $K \rightarrow \pi\pi$  transitions. During the last six years KLOE has done two precise measurements of  $\mathcal{R}_\pi$ , the final combined value for  $\mathcal{R}_\pi$  is  $2.2549 \pm 0.0054$ , a two part per mil measurement [12].

$K_S \rightarrow \pi e \nu(\gamma)$  — the  $K_S$  decays semileptonically, (meaning that leptons are present amongst its decay products) less than one per cent of the time. To pick out such decays where the event contains an unseen neutrino is non-trivial. Yet, KLOE has isolated a very pure sample of  $\sim 13\,000$  semileptonic  $K_S$  decays and accurately measured the BRs for  $K_S \rightarrow \pi^+e^-\bar{\nu}(\gamma)$  and  $K_S \rightarrow \pi^-e^+\nu(\gamma)$  [13].

The basic steps in the analysis are: tag  $K_S$  decays by the  $K_L$  crash, make a cut on the  $\pi\pi$  invariant mass (this removes 95% of the  $K_S \rightarrow \pi^+\pi^-$  decays and reduces the background-to-signal ratio to  $\sim 80:1$ ), impose several geometrical cuts to further improve the purity of the sample and, in particular, remove contamination by events with early  $\pi \rightarrow \mu\nu$  decays. Finally, stringent requirements are imposed on the particle time of flight (TOF), which very effectively separates electrons from pions and muons and allows charge assignment of the final state.

Fig. 9 shows the signal peak and the residual background in the distribution of  $\Delta_{Ep} = E_{\text{miss}} - |\mathbf{p}_{\text{miss}}|$  for the  $\pi^-e^+\nu$  channel, where  $E_{\text{miss}}$  and  $\mathbf{p}_{\text{miss}}$  are, respectively, the missing energy and momentum at the vertex, evaluated in the signal hypothesis. For signal events, the missing particle is a neutrino and  $\Delta_{Ep} = 0$ .

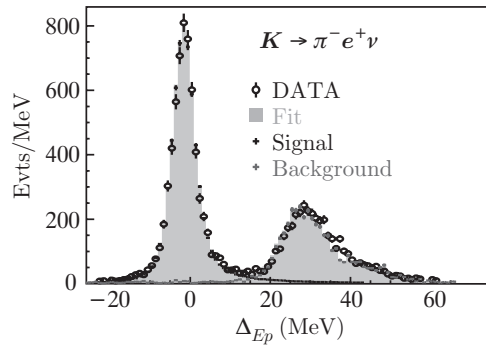


Fig. 9.  $\Delta_{Ep}$  distribution for  $K_S \rightarrow \pi^-e^+\nu$  candidates, showing signal and background.

The numbers of  $\pi e \nu$  decays for each charge state are normalized to the number of  $\pi^+ \pi^-$  events observed, resulting in the ratios in the first column of Table I. These ratios give the first measurement of the semileptonic charge asymmetry for the  $K_S$ :

$$A_S = (1.5 \pm 9.6 \pm 2.9) \times 10^{-3}.$$

Using the result for  $\mathcal{R}_\pi$  of the previous section (also in Table I), the absolute BRs for  $K_S \rightarrow \pi\pi$  and  $K_S \rightarrow \pi e \nu$  in the second column of the table are obtained.

TABLE I

KLOE measurements of  $K_S$  branching ratios.

Mode	BR(mode)/BR( $\pi^+ \pi^-$ )	BR(mode)
$\pi^+ \pi^-$	—	$(69.196 \pm 0.024 \pm 0.045)\%$
$\pi^0 \pi^0$	$1/(2.2549 \pm 0.0054)$	$(30.687 \pm 0.024 \pm 0.045)\%$
$\pi^- e^+ \nu$	$(5.099 \pm 0.082 \pm 0.039) \times 10^{-4}$	$(3.528 \pm 0.057 \pm 0.027) \times 10^{-4}$
$\pi^+ e^- \bar{\nu}$	$(5.083 \pm 0.073 \pm 0.042) \times 10^{-4}$	$(3.517 \pm 0.050 \pm 0.029) \times 10^{-4}$
$\pi e \nu$	$(10.19 \pm 0.11 \pm 0.07) \times 10^{-4}$	$(7.046 \pm 0.076 \pm 0.051) \times 10^{-4}$

**$K_S \rightarrow 3\pi^0$**  — The decay  $K_S \rightarrow 3\pi^0$  is purely CP violating. If CPT invariance holds, the BR for this decay is predicted to be  $\text{BR} \sim 1.9 \times 10^{-9}$ . In KLOE, the signature is an event with a  $K_L$  crash, six photon clusters, and no tracks from the interaction point. Background is mainly from  $K_S \rightarrow \pi^0 \pi^0$  events with two spurious clusters from splittings or accidental activity. Signal-event candidates are counted using the distribution in the plane of two  $\chi^2$ -like discriminating variables,  $\zeta_3$  and  $\zeta_2$ .  $\zeta_3$  is the quadratic sum of the residuals between the nominal  $\pi^0$  mass,  $m_{\pi^0}$ , and the invariant masses of three photon pairs formed from the six clusters present.  $\zeta_2$  is based on energy and momentum conservation in the  $\phi \rightarrow K_S K_L$ ,  $K_S \rightarrow \pi^0 \pi^0$  decay hypothesis, as well as on the invariant masses of two photon pairs.  $\zeta_3$  and  $\zeta_2$  are evaluated with the most favorable cluster pairing in each case.

From  $450 \text{ pb}^{-1}$  of data, and using the predicted distribution from an MC sample with an effective statistics of 5.3 times that of the data, KLOE obtained  $\zeta_2$  versus  $\zeta_3$  distributions. The number of predicted background counts is  $3.1 \pm 0.8 \pm 0.4$ ; while two counts in the signal box are observed in data. KLOE thus obtains the 90% C.L. limit  $\text{BR} \leq 1.2 \times 10^{-7}$ , [14], at present the most stringent limit on this BR.

### 3.5. $K_L$ decays

The KLOE measurement of the semileptonic  $K_L$  BRs [11] uses tagging to obtain absolute BRs: the presence of a  $K_L$  is tagged by observation of a  $K_S \rightarrow \pi^+\pi^-$  decay. An important point is that four modes,  $\pi^\pm e^\mp \nu$  ( $K_{e3}$ ),  $\pi^\pm \mu^\mp \nu$  ( $K_{\mu 3}$ ),  $\pi^+\pi^-\pi^0$ , and  $3\pi^0$ , account for more than 99.5% of all decays. For the first three modes, two tracks are observed in the DC, whereas for the  $3\pi^0$  mode, only photons appear in the final state. The analysis of two-track and all-neutral-particle events is, therefore, different.

Two-track events are assigned to the three channels of interest by use of a single variable: the smaller absolute value of the two possible values of  $\Delta_{\mu\pi} = |\mathbf{p}_{\text{miss}}| - E_{\text{miss}}$ , where  $\mathbf{p}_{\text{miss}}$  and  $E_{\text{miss}}$  are the missing momentum and energy in the  $K_L$  decay, respectively, and are evaluated assuming the decay particles are a pion and a muon.

Fig. 10, left, shows an example of a  $\Delta_{\mu\pi}$  distribution. A total of approximately 13 million tagged  $K_L$  decays ( $328 \text{ pb}^{-1}$ ) are used for the measurement of the BRs.

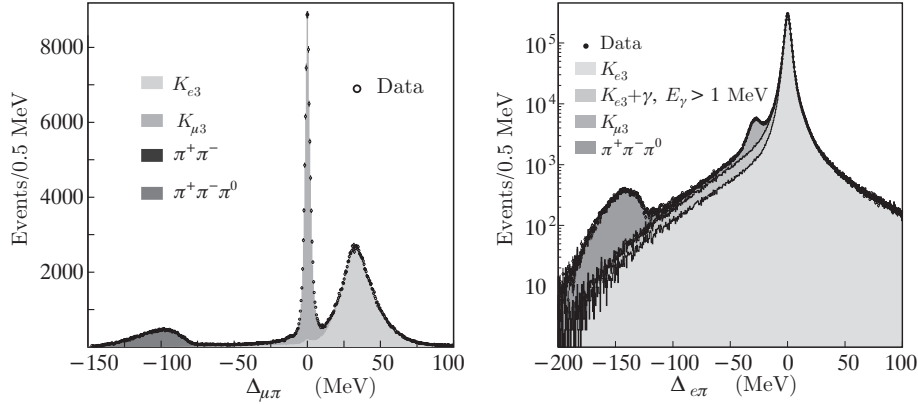


Fig. 10. Left: distribution of  $\Delta_{\mu\pi}$  for a run set. Right: distribution of  $\Delta_{e\pi}$  for events with an identified electron, for the entire data set.

The numbers of  $K_{e3}$ ,  $K_{\mu 3}$ , and  $\pi^+\pi^-\pi^0$  decays are obtained separately for each of 14 run periods by fitting the  $\Delta_{\mu\pi}$  distribution with the corresponding MC-predicted shapes. The signal extraction procedure is tested using particle-identification variables from the calorimeter.

Fig. 10, right, shows the  $\Delta_{e\pi}$  spectrum for events with identified electrons, together with the results of a fit using MC shapes. The  $K_{e3(\gamma)}$  radiative tail is clearly evident. The inclusion of radiative processes in the simulation is necessary to obtain an acceptable fit, as well as to properly estimate the fully inclusive radiative rates.

The decay  $K_L \rightarrow 3\pi^0$  is easier to identify. Detection of  $\geq 3$  photons originating at the same point is accomplished with very high efficiency (99%) and very little background (1.1%).

The errors on the absolute BRs are dominated by the uncertainty on the value of  $\tau_{K_L}$ , which enters into the calculation of the geometrical efficiency. This source of uncertainty can be all but removed (at the cost of correlating the errors among the BR measurements) by applying the constraint that the  $K_L$  BRs must add to unity. The sum of the four BRs, plus the sum of the Particle Data Group (PDG) values [8] for  $K_L$  decays to  $\pi^+\pi^-$ ,  $\pi^0\pi^0$ , and  $\gamma\gamma$  ( $\sum = 0.0036$ ), is  $1.0104 \pm 0.0018 \pm 0.0074$ .

Applying the constraint gives the results in Table II.

Constraining the BRs to add up to unity and solving for the geometrical efficiency is equivalent to determining  $\tau_{K_L}$  by the second method described in section 3.2. KLOE finds  $\tau_{K_L} = 50.72 \pm 0.17 \pm 0.33$  ns.

For the ratio  $\Gamma(K_{\mu 3})/\Gamma(K_{e 3})$ , KLOE obtains  $R_{\mu e} = 0.6734 \pm 0.0059$ . A value for comparison can be computed from the slope of the  $f_0$  form factor. We have also measured the vector form factor parameter [15].

TABLE II

KLOE measurements of  $K_L$  branching ratios.

Mode	BR	$\delta$ stat	$\delta$ syst-stat	$\delta$ syst
$\pi^\pm e^\mp \nu$	0.4007	0.0005	0.0004	0.0014
$\pi^\pm \mu^\mp \nu$	0.2698	0.0005	0.0004	0.0014
$\pi^0 \pi^0 \pi^0$	0.1997	0.0003	0.0004	0.0019
$\pi^+ \pi^- \pi^0$	0.1263	0.0004	0.0003	0.0011

### 3.6. $K^\pm$ decays

The charged kaons,  $K^\pm$ , decay mostly into  $\mu^\pm \nu$  ( $K_{\mu 2}$ ) and  $\pi^\pm \pi^0$  ( $K_{\pi 2}$ ). The semileptonic modes account for about 8% of all decays. Most dominantly, the  $K_{\mu 2}$  mode is  $\sim$  two-thirds of all  $K^\pm$  decays. It is often used as a reference for measuring other BRs, and, together with the  $K^\pm$  lifetime, provides a measurement of the decay constant  $f_K$ .

$K^+ \rightarrow \mu^+ \nu(\gamma)$  — the KLOE measurement of this BR [16] is based on the use of  $K^- \rightarrow \mu^- \bar{\nu}$  decays for event tagging. Identification of a  $K^- \rightarrow \mu^- \bar{\nu}$  decay requires the presence of a two-track vertex in the DC. The large number of  $K_{\mu 2}$  decays allows for a statistical precision of  $\sim 0.1\%$ , while setting aside a generous sample for systematic studies. The shape of the  $p^*$  distribution for signal events is obtained from a sample of control data. This distribution is used with the distributions for background sources to fit the  $p^*$  spectrum Fig. 11 (center panel). Fig. 11 (right panel) shows the spectrum

after background subtraction. In a sample of four million tagged events, KLOE finds  $\sim 865\,000$  signal events with  $225 \leq p^* \leq 400$  MeV, giving  $\text{BR}(K^+ \rightarrow \mu^+ \nu(\gamma)) = 0.6366 \pm 0.0009 \pm 0.0015$ . This measurement is fully inclusive of final-state radiation (FSR) and has a 0.27% uncertainty.

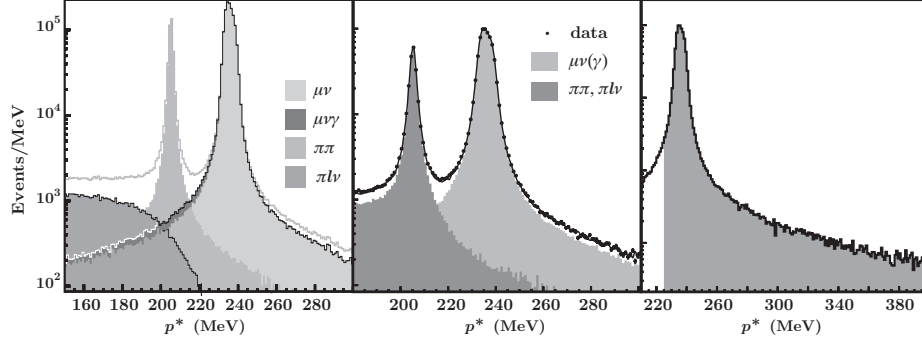


Fig. 11. Left panel: Monte Carlo spectra of  $p^*$  for  $K^+$  decays, showing contributions from various channels. Center panel: distribution of  $p^*$ . Right panel: distribution of  $p^*$  after background subtraction. The shaded area is used to count  $K^+ \rightarrow \mu^+ \nu$  events.

### 3.7. Semileptonic decays of charged kaons

The measurement is based on counting decays to each channel in samples tagged by detection of two-body decays of the other kaon. KLOE measures the semileptonic BRs separately for  $K^+$  and  $K^-$ . Therefore,  $\text{BR}(K^\pm \rightarrow \pi^0 e^\pm \nu(\gamma))$  and  $\text{BR}(K^\pm \rightarrow \pi^0 \mu^\pm \nu(\gamma))$  are each determined from four independent measurements ( $K^+$  and  $K^-$  decays tagged by  $K \rightarrow \mu\nu$  and  $K \rightarrow \pi\pi^0$ ). After removal of  $\pi^+\pi^0$  decays from the signal sample, the leptonic  $\pi^0$  is reconstructed from the two  $\gamma$ s, providing the kaon decay point. Finally, the  $m_\ell^2$  distribution for the decay lepton is reconstructed by TOF. The  $m_\ell^2$  distribution is shown in Fig. 12. The four separate determinations of each BR provide an estimate of the systematic uncertainties. The KLOE values for the BRs and their ratio  $R_{\mu e}$  are

$$\begin{aligned} \text{BR}(K_{e3}^\pm) &= (5.047 \pm 0.046_{\text{stat+tag}} \pm \sigma_{\text{syst}}), \\ \text{BR}(K_{\mu 3}^\pm) &= (3.310 \pm 0.040_{\text{stat+tag}} \pm \sigma_{\text{syst}}), \\ R_{\mu e} &= 0.656 \pm 0.008. \end{aligned}$$

These results are preliminary, awaiting final determination of certain systematic uncertainties, still in progress [17].

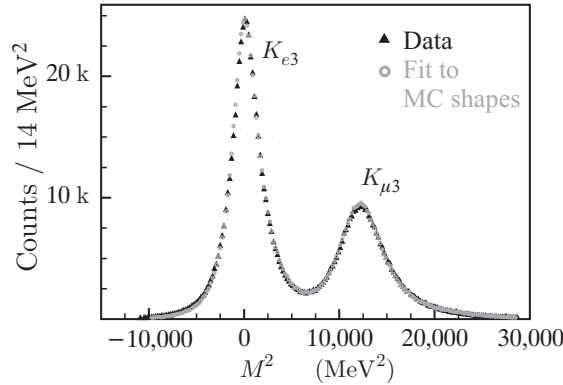


Fig. 12. Distribution of  $m_\ell^2$ , for events selected as  $K_{\ell 3}^\pm$  decays. Also shown is a fit to MC distributions for signal and background.

#### 4. $|V_{us}|$

In the Standard Model, the quark weak charged current is

$$J_\alpha^+ = (\bar{u} \ \bar{c} \ \bar{t}) \gamma_\alpha (1 - \gamma_5) \mathbf{V} \begin{pmatrix} d \\ s \\ b \end{pmatrix},$$

where  $\mathbf{V}$  is a  $3 \times 3$  unitary matrix introduced by Kobayashi and Maskawa [18] expanding on the original suggestion by Cabibbo [19]. The unitarity condition ( $\mathbf{V}^\dagger \mathbf{V} = 1$ ) is required by the assumption of universality of the weak interactions of leptons and quarks and the absence of flavor-changing neutral currents. The realization that a precise test of CKM unitarity can be obtained from the first-row constraint  $|V_{ud}|^2 + |V_{us}|^2 + |V_{ub}|^2 = 1$  (with  $|V_{ub}|^2$  negligible) has sparked a new interest in good measurements of quantities related to  $|V_{us}|$ . As we discuss in the following  $|V_{us}|$  can be determined using semileptonic kaon decays; the experimental inputs are the BRs, lifetimes, and form-factor slopes. Both neutral ( $K_S$  or  $K_L$ ) and charged kaons may be used and provide independent measurements.

KLOE is unique in that it is the only experiment that can by itself measure the complete set of experimental inputs for the calculation of  $|V_{us}|$  using both charged and neutral kaons. Recall that we are at a  $\phi$ -factory thus are especially suited for measurements of the  $K_L$  and  $K^\pm$  lifetimes. In addition, KLOE is the only experiment that can measure  $K_S$  BRs at the sub-percent level.

#### 4.1. Semileptonic kaon decays

The semileptonic kaon decay rates still provide the best means for the measurement of  $|V_{us}|$  because only the vector part of the weak current contributes to the matrix element  $\langle \pi | J_\alpha | K \rangle$ . For vector transitions, the Ademollo–Gatto theorem [20] ensures that SU(3) breaking appears only to second order in  $m_s - m_{u,d}$ . Still one has to properly account for radiative correction, SU(2) and SU(3) corrections, [21]. Finally, the matrix element of the weak vector current contains two form factor, FF, which reflect on the value of the phase space integral. For this last point we have no theoretical help but we can measure their shape experimentally. The semileptonic decay rates, fully inclusive of radiation, are given by

$$\begin{aligned} \Gamma_i(K_{e3, \mu 3}) = & |V_{us}|^2 \frac{C_i^2 G^2 M^5}{768 \pi^3} S_{EW} \left( 1 + \delta_{i, \text{em}} + \delta_{i, \text{SU}(2)} \right) \\ & \times \left| f_+^{K^0}(0) \right|^2 I_{e3, \mu 3}. \end{aligned} \quad (2)$$

In the above expression,  $i$  indexes  $K^0$  and  $K^\pm$ .  $S_{EW}$  is the universal short-distance radiative correction factor and the  $\delta$  terms are all the other correction mentioned. The phase space integrals  $I_{e3, \mu 3}$  require knowledge of the FF parameters. The numerical factor in the denominator of Eq. (2),  $768 = 3 \times 2^8$ , is chosen in such a way that  $I = 1$  when the masses of all final-state particles vanish. For  $K_{e3}$ ,  $I \approx 0.56$  and for  $K_{\mu 3}$ ,  $I \approx 0.36$ .

The biggest uncertainty at present is in the value of the vector form factor at zero momentum transfer,  $f_+^{K^0}(0)$  in Eq. (2). Progress is expected from lattice calculations. It has, therefore, become customary to extract from data and Eq. (2) the value of  $\kappa = f_+^{K^0}(0) |V_{us}|$ , which contains all the measured parameters described above.

KLOE finds  $\kappa = 0.2157 \pm 0.0006$ ,  $0.2163 \pm 0.0008$ ,  $0.2155 \pm 0.0014$ ,  $0.2171 \pm 0.0021$ ,  $0.2150 \pm 0.0028$ , respectively, for  $K_L(e3)$ ,  $K_L(\mu 3)$ ,  $K_S(e3)$ ,  $K^\pm(\mu 3)$ ,  $K^\pm(e3)$  using exclusively KLOE data except for the slope of the scalar FF,  $\lambda_0$  [22], which we are currently measuring and the  $K_S$  lifetime which is very well known since a long time [8]. The above value are quite consistent with each other. The weighted average is  $\langle \kappa \rangle = 0.2160 \pm 0.005$ . This value is in agreement with more limited results from other experiments. It compares well with the value  $\sqrt{1 - |V_{ud}|^2} \times f_+^{K^0}(0) = 0.2187 \pm 0.0022$ , using  $f_+^{K^0}(0) = 0.961 \pm 0.008$  (Leutwyler and Ross [21]) and  $|V_{ud}| = 0.9740 \pm 0.0003$  (Marciano and Sirlin, [21]). In conclusion, Unitarity of the CKM mixing matrix, requiring  $|V_{ud}|^2 + |V_{us}|^2 = 1.0$  to better than 0.00002, given the smallness of  $|V_{ub}|$ , is essentially satisfied.

#### 4.2. $K \rightarrow \mu\nu$ decays

Reliable lattice quantum chromodynamics (QCD) results have recently become available and are rapidly improving [23]. The availability of precise values for the pion- and kaon-decay constants  $f_\pi$  and  $f_K$  allows the use of a relation between  $\Gamma(K_{\mu 2})/\Gamma(\pi_{\mu 2})$  and  $|V_{us}|^2/|V_{ud}|^2$ , with the advantage that lattice-scale uncertainties and radiative corrections largely cancel out in the ratio [24]:

$$\frac{\Gamma(K_{\mu 2}(\gamma))}{\Gamma(\pi_{\mu 2}(\gamma))} = \frac{|V_{us}|^2}{|V_{ud}|^2} \frac{f_K^2}{f_\pi^2} \frac{m_K (1 - m_\mu^2/m_K^2)^2}{m_\pi (1 - m_\mu^2/m_\pi^2)^2} (0.9930 \pm 0.0035). \quad (3)$$

All information about the unitarity of the CKM matrix, as verified on the first row, is represented graphically in Fig. 13.

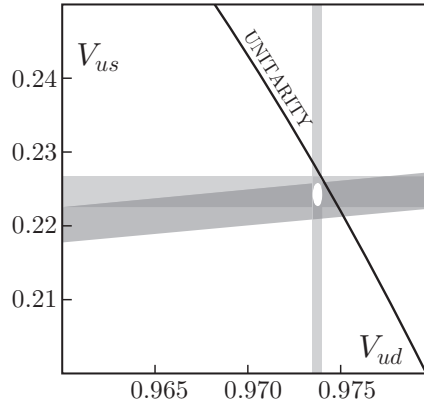


Fig.13. The vertical band gives the value of  $|V_{ud}|$  as measured in nuclear  $\beta$ -decay. The horizontal band gives  $|V_{us}|$  from semileptonic kaon decays, using  $f_+^{K^0}(0)=0.96\pm0.008$ . The slightly inclined band follows from Eq. (1) and the KLOE result for  $\text{BR}(K_{\mu 2})$ . Unitarity is represented by an arc of circle. The white ellipses is the  $1\sigma$  contour from a fit to all data.

### 5. Quantum interferometry

As stated in section 2.7, the neutral kaon pair  $\phi \rightarrow K^0 \bar{K}^0$  are produced in a pure quantum state with  $J^{\text{PC}}=1^{--}$ . We evolve the initial state in Eq. (1) in time, project to any two possible final states  $f_1$  and  $f_2$ , take the modulus squared, and integrate over all  $t_1$  and  $t_2$  for fixed  $\Delta t = t_1 - t_2$  to obtain (for  $\Delta t > 0$ , with  $\Gamma \equiv \Gamma_L + \Gamma_S$ )

$$I_{f_1, f_2}(\Delta t) = \frac{1}{2\Gamma} \left| \langle f_1 | K_S \rangle \langle f_2 | K_S \rangle \right|^2 \left[ |\eta_1|^2 e^{-\Gamma_L \Delta t} + |\eta_2|^2 e^{-\Gamma_S \Delta t} - 2(1 - \zeta) |\eta_1| |\eta_2| e^{-(\Gamma_L + \Gamma_S) \Delta t / 2} \cos(\Delta m \Delta t + \phi_2 - \phi_1) \right]. \quad (4)$$

The last term is due to interference between the decays to states  $f_1$  and  $f_2$  and  $\zeta = 0$  in quantum mechanics. Fits to the  $\Delta t$  distribution provide measurements of the magnitudes and phases of the parameters  $\eta_i = \langle f_i | K_L \rangle / \langle f_i | K_S \rangle$ , as well as of the  $K_L$ – $K_S$  mass difference  $\Delta m$  and the decay rates  $\Gamma_L$  and  $\Gamma_S$ .

Such fits also allow tests of fundamental properties of quantum mechanics. For example, the persistence of quantum-mechanical coherence can be tested by choosing  $f_1 = f_2$ . In this case, because of the antisymmetry of the initial state and the symmetry of the final state, there should be no events with  $\Delta t = 0$ . Using the 2001–2002 data, KLOE has conducted a preliminary analysis of the  $\Delta t$  distribution for  $K_S K_L \rightarrow \pi^+ \pi^- \pi^+ \pi^-$  events that establishes the feasibility of such tests [25]. The  $\Delta t$  distribution is fit with a function of the form of Eq. (4), including the experimental resolution and a peak from  $K_L \rightarrow K_S$  regeneration in the beam pipe. The results are shown in Fig. 14. Observation of  $\zeta \neq 0$  would imply loss of quantum coherence. The value of  $\zeta$  depends on the basis,  $K^0 - \bar{K}^0$  or  $K_S - K_L$  used in the analysis. Using the  $K^0 - \bar{K}^0$  basis we find  $\zeta = (0.1 \pm 0.2 \pm 0.04) \times 10^{-5}$  *i.e.* no violation of quantum mechanics.

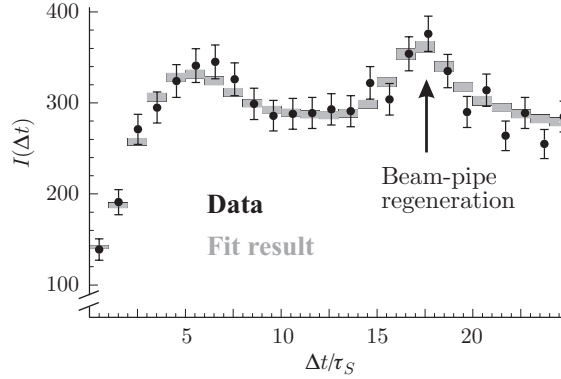


Fig. 14.  $\Delta t$  distribution for  $\phi \rightarrow K_S K_L \rightarrow \pi^+ \pi^- \pi^+ \pi^-$  events.

## 6. Test of CPT

The three discrete symmetries of quantum mechanics, charge conjugation (C), parity (P) and time reversal (T) are known to be violated in nature, both singly and in pairs. Only CPT appears to be an exact symmetry of nature. Exact CPT invariance holds in quantum field theory which assumes Lorentz invariance (flat space), locality and unitarity [26]. These assumptions could be violated at very large energy scales, where quantum gravity cannot be ignored [27]. Testing the validity of CPT invariance probes the most fundamental assumptions of our present understanding of particles

and their interactions. The neutral kaon system offers unique possibilities for the study of CPT invariance. From the requirement of unitarity, Bell and Steinberger have derived a relation, the so called Bell–Steinberger relation (BSR) [28]. The BSR relates a possible violation of CPT invariance ( $m_{K^0} \neq m_{\bar{K}^0}$  and/or  $\Gamma_{K^0} \neq \Gamma_{\bar{K}^0}$ ) in the time-evolution of the  $K^0 - \bar{K}^0$  system to the observable CP-violating interference of  $K_S$  and  $K_L$  decays into the same final state  $f$ , in terms of CP- and CPT-violating parameters  $\text{Re}\epsilon$  and  $\text{Im}\delta$ . Recently we succeeded in improving the determination of those two parameters using KLOE results. Specifically we benefitted from our new precise measurement of the branching ratio for  $K_L$  decays to  $\pi^+\pi^-$  [29], which is relevant for the determination of  $\text{Re}\epsilon$ . We improved the upper limit on  $\text{BR}(K_S \rightarrow \pi^0\pi^0\pi^0)$  [14], which is necessary to improve the accuracy on  $\text{Im}\delta$ . Finally we obtained the first measurement of the charge asymmetry  $A_S$  for  $K_S$  semileptonic decays. The latter allowed us to determine the direct contribution from semileptonic channels *without assuming unitarity*. Our study resulted in narrowing the mass difference to  $(-5.3 \leq m_{K^0} - m_{\bar{K}^0} \leq 6.3) \times 10^{-19}$  GeV 95% CL, see Fig. 15, a factor of two better than previous limits [30].

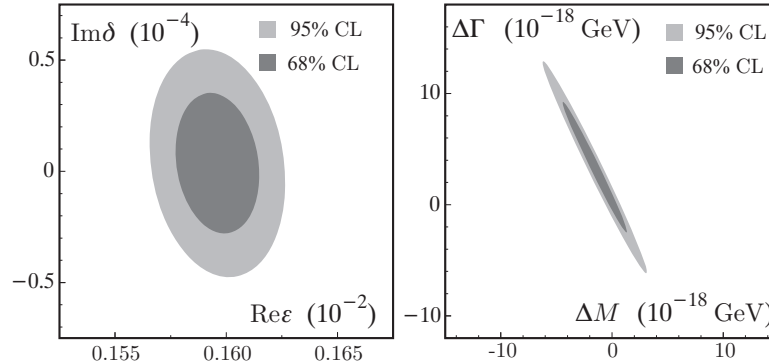


Fig. 15. Left: allowed region at 68% and 95% C.L. in the  $\text{Re}\epsilon$ ,  $\text{Im}\delta$  plane. Right: allowed region at 68% and 95% C.L. in the  $\Delta M$ ,  $\Delta\Gamma$  plane.

## 7. $\phi$ radiative decays

It is serendipitous that while on the  $\phi$  peak kaons are produced furiously, it also happens that, true its name, DAΦNE is a  $\phi$ -factory. These  $\phi$  mesons, by electromagnetic transitions ( $\phi \rightarrow \text{meson} + \gamma$ ) to other mesons, result in a great profusion of lighter scalar and pseudoscalar mesons. The transition rates are strongly dependent on the wave function of the final-state meson. They also depend on its flavor content, because the  $\phi$  is a nearly pure  $s\bar{s}$  state and because there is no photon–gluon coupling. These radiative  $\phi$  decays are unique probes of meson properties and structure. This hadron

source, coupled with KLOE's great versatility, allowed KLOE to perform many hadronic experiments, with far greater precision than has been done elsewhere before.

In addition, initial-state radiation (ISR) lowers the effective collision energy squared from  $s$  to  $s_\pi = (s - 2E_\gamma\sqrt{s})$ , providing access to hadronic states of mass  $\sqrt{s_\pi}$  from threshold to  $m_\phi$ . KLOE has exploited ISR to measure the  $e^+e^- \rightarrow \pi^+\pi^-$  cross-section over this entire energy range without changing the DAΦNE energy [31]. In this paper we have no space to delve into this last fascinating and somewhat fractious topic. Similarly, due to space constraint, we will limit ourselves to mentioning only a handful of the radiative decays measurements, just enough to give a taste of hadron physics with KLOE.

**The  $\eta$  meson** — the BR for the decay  $\phi \rightarrow \eta\gamma$  is 1.3%. In  $2.5 \text{ fb}^{-1}$  of KLOE data, there are 100 million  $\eta$  mesons, identified clearly by their recoil against a photon of  $E = 363 \text{ MeV}$ . KLOE has used the  $\eta$  meson to test discrete symmetry laws in several ways. (1) The symmetries of the Dalitz plot for  $\eta \rightarrow \pi^+\pi^-\pi^0$  decays provide tests of charge-conjugation invariance. KLOE has made such plots with about 1.4 million events and obtain violation limits of the order of  $0.002 \pm 0003$ . (2) The decay  $\eta \rightarrow 3\gamma$  violates  $C$ , while the decay  $\eta \rightarrow \pi^+\pi^-$  violates both  $P$  and  $CP$ . KLOE has conducted a search for the decay  $\eta \rightarrow 3\gamma$  using  $410 \text{ pb}^{-1}$  and obtained the limit  $\text{BR}(\eta \rightarrow 3\gamma) \leq 1.6 \times 10^{-5}$  at 90% C.L., the most stringent obtained to date [32]. (3) KLOE has also searched for evidence of the decay  $\eta \rightarrow \pi^+\pi^-$  in the tail of the  $M_{\pi\pi}$  distribution for  $e^+e^- \rightarrow \pi^+\pi^-\gamma$  events in which the photon is emitted at large polar angles ( $\theta > 45^\circ$ ). No peak is observed in the distribution of  $M_{\pi\pi}$  in the vicinity of  $m_\eta$ . The corresponding limit is  $\text{BR}(\eta \rightarrow \pi^+\pi^-) \leq 1.3 \times 10^{-5}$  at 90% C.L. [33], which is more stringent than the previous limit by a factor of 25.

The decay  $\eta \rightarrow \pi^0\gamma\gamma$  is particularly interesting in chiral perturbation theory. There is no  $\mathcal{O}(p^2)$  contribution, and the  $\mathcal{O}(p^4)$  contribution is small. At KLOE, the decay can be reconstructed with full kinematic closure and without complications from certain backgrounds present in fixed-target experiments, such as  $\pi^-p \rightarrow \pi^0\pi^0n$ . Using one fifth of its data, KLOE has obtained the preliminary result  $\text{BR}(\eta \rightarrow \pi^0\gamma\gamma) = (8.4 \pm 2.7 \pm 1.4) \times 10^{-5}$ , which is in agreement with several  $\mathcal{O}(p^6)$  chiral perturbation theory calculations discussed in a recent  $\eta$  workshop [34]. The final measurement using the complete set of data is expected in 2007.

**The  $\eta'$  meson** — the magnitude of  $\text{BR}(\phi \rightarrow \eta'\gamma)$  is a probe of the  $s\bar{s}$  content of the  $\eta'$ . Furthermore, the ratio  $R_\phi \equiv \text{BR}(\phi \rightarrow \eta'\gamma)/\text{BR}(\phi \rightarrow \eta\gamma)$  can be related to the pseudoscalar mixing angle  $\varphi_P$  in the basis  $\{|u\bar{u} + d\bar{d}\rangle/\sqrt{2}, |s\bar{s}\rangle\}$ , offering an important point of comparison for the description of the  $\eta$ - $\eta'$  mixing in extended chiral perturbation theory [35].

At KLOE the  $\phi \rightarrow \eta'\gamma$  decay is identified in either the charged pion channel where  $\eta' \rightarrow \eta\pi^+\pi^-$  with  $\eta \rightarrow \gamma\gamma$  or with  $\eta \rightarrow 3\pi^0$ , or in the neutral pion channel  $\eta' \rightarrow \eta\pi^0\pi^0$  with  $\eta \rightarrow \pi^+\pi^-\pi^0$ . The  $\phi \rightarrow \eta\gamma$  decay is identified in the channel in which  $\eta \rightarrow \pi^+\pi^-\pi^0$ . To date, from study of one fifth of the KLOE data collected, we obtained  $R_\phi = (4.77 \pm 0.09_{\text{stat}} \pm 0.19_{\text{sys}}) \times 10^{-3}$  from which we derive  $\text{BR}(\phi \rightarrow \eta'\gamma) = (6.20 \pm 0.11_{\text{stat}} \pm 0.25_{\text{sys}}) \times 10^{-5}$ . Scant knowledge of intermediate branching ratios prevents us to benefit from having twentyfold statistics over our previous BR determination [36]. In the hypothesis of no gluonium content we extract the pseudo-scalar mixing angle in the quark-flavor basis  $\varphi_P = (41.4 \pm 0.3_{\text{stat}} \pm 0.7_{\text{sys}} \pm 0.6_{\text{th}})^\circ$ . Combining our  $R_\phi$  result with other experimental constraints, we estimate the gluonium fractional content of  $\eta'$  meson as  $Z^2 = 0.14 \pm 0.04$  and the mixing angle  $\varphi_P = (39.7 \pm 0.7)^\circ$  [37].

### 7.1. Scalar mesons: $f_0(980)$ and $a_0(980)$

The compositions of the five scalar mesons with masses below 1 GeV are not well understood. In fact, a detailed proposal of how to elucidate their nature using KLOE at DAΦNE was one of the first papers J.L.F. had written, after her arrival to LNF in 1991 [38]. Theoretical models have proliferated greatly, we only pick two which are illustrated below. KLOE has now collected literally millions of such decays. We not only measure branching ratios, we can obtain a very densely populated Dalitz plot. The two dimensional Dalitz plot density, subdivided into fine cells, can be fit to theoretical models. As of this writing, some theoretical models are so over encumbered with parameters that the physical meaning of several are opaque, and render fits to them difficult to interpret. So here we leave out all detailed discussions of the recent KLOE fits.

**Branching Ratios:** the branching ratio for the decays  $\phi \rightarrow f_0\gamma \rightarrow \pi\pi\gamma$  and  $\phi \rightarrow a_0\gamma \rightarrow \eta\pi^0\gamma$  are suppressed unless the  $f_0$  and  $a_0$  have significant  $s\bar{s}$  content. The BRs for these decays are estimated to be on the order of  $10^{-4}$  if the  $f_0$  and  $a_0$  are  $qq\bar{q}\bar{q}$  states (in which case they contain an  $s\bar{s}$  pair), or on the order of  $10^{-5}$  if the  $f_0$  and  $a_0$  are conventional  $q\bar{q}$  states. If the  $f_0$  and  $a_0$  are  $K\bar{K}$  molecules, the BR estimates are sensitive to assumptions about the spatial extension of these states.

**Invariant Mass Distributions:**  $\pi\pi$  and  $\eta\pi^0$  invariant-mass distributions can shed light on the nature of the  $f_0$  and  $a_0$  because fits to the distributions provide estimates of the couplings of these mesons to the  $\phi$  and/or to the final-state particles. To make fits one necessarily assumes a specific model for the decay mechanism. Because of the proximity of the  $f_0$  and  $a_0$  masses to the  $K\bar{K}$  threshold, and because these mesons are known to couple strongly to  $K\bar{K}$ , the kaon-loop model, Fig. 16, is often used [39].

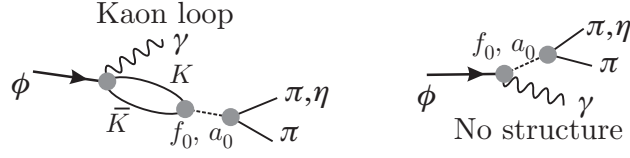


Fig. 16. Amplitudes used to compute the  $\pi\pi$  and  $\eta\pi^0$  mass spectra for  $\phi \rightarrow S\gamma$ .

The expression for the rate for E1  $\phi \rightarrow S\gamma$  transitions ( $S = f_0$  or  $a_0$ ) contains a factor  $E_\gamma^3$  (where  $E_\gamma$  is the energy of the radiated photon), as required by considerations of phase space and gauge invariance. As a result, the invariant-mass distributions in  $\phi \rightarrow S\gamma$  decays are cut off above  $m_\phi$  and develop a long tail toward lower mass values (see Fig. 17, right). The fit results, therefore, depend strongly on the scalar meson masses and widths.  **$\phi \rightarrow \pi^0\pi^0\gamma$  and  $\phi \rightarrow \eta\pi^0\gamma$**  — the first KLOE studies of the decays  $\phi \rightarrow \pi^0\pi^0\gamma$  [40] and  $\phi \rightarrow \eta\pi^0\gamma$  [41] were performed with the  $17\text{pb}^{-1}$  of data collected in 2000. All BR's quoted therein are in agreement with, but are much more precise than previous measurements.

The amplitudes contributing to  $\phi \rightarrow \pi^0\pi^0\gamma$  include  $\phi \rightarrow S\gamma$  (with  $S = f_0$  or  $\sigma$ ) and  $\phi \rightarrow \rho^0\pi^0$  (with  $\rho^0 \rightarrow \pi^0\gamma$ ). The  $M_{\pi\pi}$  distribution was fit with a function including terms describing the contribution from  $\phi \rightarrow S\gamma$ , that from  $\phi \rightarrow \rho\pi$ , and their interference. The value obtained for  $\text{BR}(\phi \rightarrow \pi^0\pi^0\gamma)$  was  $(1.09 \pm 0.03 \pm 0.05) \times 10^{-4}$ . In the  $a_0$  case, the amplitudes contributing are  $\phi \rightarrow a_0\gamma$  and  $\phi \rightarrow \rho^0\pi^0$ , with  $\rho^0 \rightarrow \eta\gamma$ . In KLOE analyses, final states corresponding to two different  $\eta$  decay channels were studied:  $\eta \rightarrow \gamma\gamma$  ( $5\gamma$  final state) and  $\eta \rightarrow \pi^+\pi^-\pi^0$  ( $\pi^+\pi^-\pi^0 5\gamma$  final state). The  $M_{\eta\pi}$  distributions for each sample were fit simultaneously with a function analogous to that discussed above. The values obtained for  $\text{BR}(\phi \rightarrow \eta\pi^0\gamma)$  using the  $5\gamma$  and  $\pi^+\pi^-\pi^0 5\gamma$  samples were  $(8.51 \pm 0.51 \pm 0.57) \times 10^{-5}$  and  $(7.96 \pm 0.60 \pm 0.40) \times 10^{-5}$ , respectively.

The analyses of the  $\phi \rightarrow \pi^0\pi^0\gamma$  and  $\phi \rightarrow \eta\pi^0\gamma$  decays based on a later data set, benefit from an increase in statistics by a factor of  $\sim 30$  such that one could eschew background removal using severe cuts which could introduce biases, and plot all events with the same topology in Dalitz plots. In such cases one fits the whole Dalitz plots by correctly modelling all channels in the MC, fold in cell by cell efficiencies, then extract the relative fraction of each channel and relevant parameters, by fitting to theoretical models. In particular, we fit to both 1, the much, much improved  $k$ -loop model [42], and also 2, to the no-structure model [43] illustrated in Fig. 16; (right panel). At present since the interpretations of some parameters, as well as the stability of some theoretical fits, are under discussion between KLOE and the theorists, we only quote here the BR to  $\phi \rightarrow \pi^0\pi^0\gamma$  [45]:

$$\text{BR}(\phi \rightarrow S\gamma \rightarrow \pi^0\pi^0\gamma) = \left(1.07^{+0.01}_{-0.04}(\text{fit}) \begin{smallmatrix} +0.04 \\ -0.02 \end{smallmatrix}(\text{syst}) \begin{smallmatrix} +0.06 \\ -0.05 \end{smallmatrix}(\text{mod})\right) \times 10^{-4}.$$

$\phi \rightarrow \pi^+\pi^-\gamma$  — KLOE has also published a study of the decay  $\phi \rightarrow f_0\gamma \rightarrow \pi^+\pi^-\gamma$  [44]. The  $f_0$ 's charged mode was extremely difficult to identify because only a small fraction of the  $e^+e^- \rightarrow \pi^+\pi^-\gamma$  events involve the  $f_0$ ; the principal contributions are from events in which the photon is from ISR or FSR. The analysis is performed on the  $M_{\pi\pi}$  distribution for events with large photon polar angle where the ISR contribution is much reduced. The  $M_{\pi\pi}$  distribution was fit with a function composed of analytic expressions describing the ISR, FSR,  $\rho\pi$  contributions and two terms that describe the decay  $\phi \rightarrow S\gamma \rightarrow \pi\pi\gamma$  and its interference with FSR which could be constructive or destructive.

Fig. 17, left, shows the  $M_{\pi\pi}$  distribution, with the result of the kaon-loop fit superimposed. The overall appearance of the distribution is dominated by the radiative return to the  $\rho$ ; the  $f_0$  appears as the peak-like structure in the region 900–1000 MeV. Fig. 17, right, shows the data in this mass region, with the ISR, FSR, and  $\rho\pi$  terms subtracted.

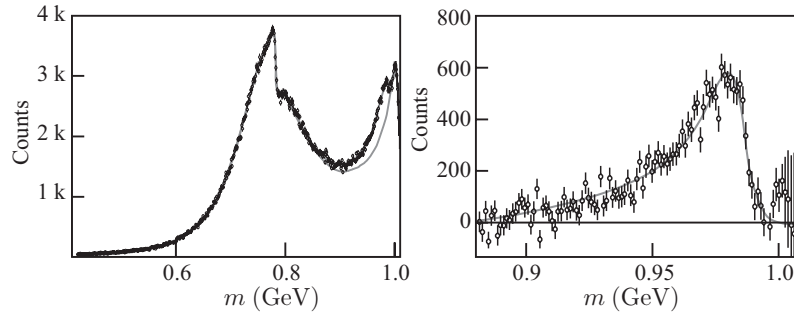


Fig. 17. Left:  $M_{\pi\pi}$  distribution for large-photon-angle  $\pi^+\pi^-\gamma$  events from KLOE. Fits with and without the  $f_0$  contribution are shown. Right: distribution in the region of the  $f_0$ , with the initial-state radiation, final-state radiation, and  $\rho\pi$  contributions subtracted.

Both the kaon-loop and no-structure fits strongly prefer destructive interference between the  $S\gamma$  and FSR amplitudes. The kaon-loop fit gives coupling values in reasonable agreement with those obtained from the fit to the KLOE  $\phi \rightarrow \pi^0\pi^0\gamma$  data discussed above. Integrating the appropriate terms of the fit functions gives values for  $\text{BR}(\phi \rightarrow f_0\gamma)$  in the neighborhood of  $3 \times 10^{-4}$ .

We thank the organizers of The Final Euridice Meeting at Kazimierz, August 2006, Lia Panchieri and Maria Krawczyk, for inviting us to contribute a pedagogical paper on KLOE in their proceedings. This is a token of our appreciation of the almost decade-long symbiosis between Euridice, Eurodaphne, and KLOE.

We hope that our fellow KLOE collaborators forgive us for our simplified discussion of their hard and elegant labors. Finally, one of us, JLF, wants especially to thank Caterina Bloise for representing KLOE at Lia Fest which celebrated so joyfully our friendship and collaborations.

## REFERENCES

- [1] Preprint LNF-90/031(R), (1990); <http://www.lnf.infn.it/sis/preprint>.
- [2] M. Adinolfi *et al.*, [KLOE Collab.], *Nucl. Instrum. Methods* **A488**, 51 (2002).
- [3] M. Adinolfi *et al.*, [KLOE Collab.], *Nucl. Instrum. Methods* **A482**, 364 (2002).
- [4] M. Adinolfi *et al.*, [KLOE Collab.], *Nucl. Instrum. Methods* **A492**, 134 (2002).
- [5] F. Ambrosino *et al.*, [KLOE Collab.], *Eur. Phys. J.* **C47**, 589 (2006).
- [6] A. Aloisio *et al.*, [KLOE Collab.], *Nucl. Instrum. Methods* **A516**, 288 (2004).
- [7] F. Ambrosino *et al.*, [KLOE Collab.], *Nucl. Instrum. Methods* **A534**, 403 (2004).
- [8] W.-M. Yao *et al.*, [Particle Data Group], *J. Phys. G* **33**, 1 (2006).
- [9] F. Ambrosino *et al.*, [KLOE Collab.], *Phys. Lett.* **B608**, 199 (2005).
- [10] F. Ambrosino *et al.*, [KLOE Collab.], *Phys. Lett.* **B626**, 15 (2005).
- [11] F. Ambrosino *et al.*, [KLOE Collab.], *Phys. Lett.* **B632**, 43 (2006).
- [12] A. Aloisio *et al.*, [KLOE Collab.], *Phys. Lett.* **B537**, 21 (2002); F. Ambrosino *et al.*, [KLOE Collab.], *Eur. Phys. J.* **C48**, 767 (2006).
- [13] F. Ambrosino *et al.*, [KLOE Coll.], *Phys. Lett.* **B535**, 37 (2002); *Phys. Lett.* **B636**, 173 (2006).
- [14] F. Ambrosino *et al.*, [KLOE Collab.], *Phys. Lett.* **B619**, 61 (2005).
- [15] F. Ambrosino *et al.*, [KLOE Collab.], *Phys. Lett.* **B636**, 166 (2006).
- [16] F. Ambrosino *et al.*, [KLOE Collab.], *Phys. Lett.* **B632**, 76 (2006).
- [17] F. Ambrosino *et al.*, [KLOE Collab.], *PoS HEP2005*, 287 (2006).
- [18] M. Kobayashi, T. Maskawa, *Prog. Theor. Phys.* **652**, 49 (1973).
- [19] N. Cabibbo, *Phys. Rev. Lett.* **531**, 10 (1963).
- [20] M. Ademollo R. Gatto, *Phys. Rev. Lett.* **264**, 13 (1964).
- [21] A. Sirlin, *Rev. Mod. Phys.* **573**, 50 (1978); *Nucl. Phys.* **B83**, 196 (1982); H. Leutwyler, M. Roos, *Z. Phys.* **C91**, 25 (1984); V. Cirigliano *et al.*, *Eur. Phys. J.* **C21**, 23 (2002); W.J. Marciano, A. Sirlin, *Phys. Rev. Lett.* **96**, 032002 (2006).
- [22] There is still some confusion about the value of  $\lambda_0$ . We use preliminary values from CKM06, Nagoya.
- [23] C.T.H. Davies, *et al.*, *Phys. Rev. Lett.* **92**, 022001 (2004).
- [24] W.J. Marciano, *Phys. Rev. Lett.* **93**, 231803 (2004).

- [25] F. Ambrosino *et al.*, [KLOE Collab.], *Phys. Lett.* **B642**, 315 (2006).
- [26] G. Lueders, *Annals Phys.* **2**, 1 (1957) [*Annals Phys.* **281**, 1004 (2000)].
- [27] See *e.g.* V.A. Kostelecky, R. Lehnert, *Phys. Rev.* **D63**, 065008 (2001); N. E. Mavromatos, *AIP Conf. Proc.* **796**, 13 (2005).
- [28] J.S. Bell, J. Steinberger, Proc. Oxford Int. Conf. on Elementary Particles (1965).
- [29] F. Ambrosino *et al.*, [KLOE Collab.], *Phys. Lett.* **B638**, 140 (2006).
- [30] F. Ambrosino *et al.*, [KLOE Collab.], *J. High Energy Phys.* **0612**, 011 (2006).
- [31] A. Aloisio *et al.*, [KLOE Collab.], *Phys. Lett.* **B606**, 12 (2005).
- [32] A. Aloisio *et al.*, [KLOE Collab.], *Phys. Lett.* **B591**, 49 (2004).
- [33] F. Ambrosino *et al.*, [KLOE Collab.], *Phys. Lett. B* **606**, (2005) 276.
- [34] Eta Physics Handbook, J. Bijnens, G. Galt, B.M.K. Nefkens, Eds., Proc. of Workshop Eta Physics, Uppsala 2001. *Phys. Scripta* **T99**, (2002).
- [35] Th. Feldmann, *Int. J. Mod. Phys.* **A159**, 15 (2000).
- [36] A. Aloisio *et al.*, [KLOE Collab.], *Phys. Lett.* **B541**, 45 (2002).
- [37] Ambrosino F, *et al.*, [KLOE Collab.], [hep-ex/0612029](#), submitted to *Phys. Lett. B*.
- [38] P.J. Franzini, W. Kim, J. Lee-Franzini, *Phys. Lett.* **B287**, 259 (1992).
- [39] N.N. Achasov, V.N. Ivanchenko, *Nucl. Phys.* **B315**, 465 (1989).
- [40] A. Aloisio *et al.*, [KLOE Collab.], *Phys. Lett.* **B537**, 21 (2002).
- [41] A. Aloisio *et al.*, [KLOE Collab.], *Phys. Lett.* **B536**, 209 (2002).
- [42] N.N. Achasov, A.V. Kiselev, *Phys. Rev.* **D73**, 054029 (2006).
- [43] G. Isidori, *et al.*, *J. High Energy Phys.* **0605**, 04 (2006)9.
- [44] F. Ambrosino *et al.*, [KLOE Collab.], *Phys. Lett.* **B634**, 148 (2006).
- [45] F. Ambrosino *et al.*, [KLOE Collab.] [hep-ex/0609009](#), submitted to *Eur. Phys. J. C*.